Efficiency of a Constant-Area, Adiabatic Tip, Heat Pipe Fin

W. J. Bowman,* T. W. Moss,† D. Maynes,‡
and K. A. Paulson†
Brigham Young University, Provo, Utah 84602

Introduction

THE efficiencies of a solid, constant-area (standard) fin and a geometrically similar fin with an internal heat pipe (heat pipe fin) were investigated. Analytical expressions for heat pipe fin temperature distribution and efficiency were derived for the case where the heat pipe is extended (inserted) into the object being cooled. The results are compared to the case where the heat pipe is simply flush mounted against the object. These results are useful for comparing heat pipe fins to standard fins. They provide a simple method of evaluating the feasibility of using heat pipe fins in an application before more expensive and time-consuming heat pipe design methods are used. Also, experiments were conducted to test the accuracy of the analytical results. Both the inserted and flush-mounted heat pipe fin cases were studied. Within the uncertainty of experimental data, the analytical and empirical data yield the same results.

Background: Flush-Mounted Heat Pipe Fin

Bowman et al.[1] derived analytical expressions for heat pipe fin temperature distributions and efficiencies and compared them to the values for standard fins. Their model assumed a uniform cross section along the length of the fin with an adiabatic tip condition. The convection coefficients on the inside (associated with evaporation and condensation) and on the outside of the fin were considered constant. The heat pipe was flush mounted against the object (Fig. 1). Neglecting radiation, assuming steady state, and assuming temperature varies only in the x direction, conservation of energy applied to a differential element of the heat pipe wall was shown to be

$$kA_w \frac{\partial^2 T}{\partial x^2} - h_o P_o (T - T_\infty) - h_i P_i (T - T_v) = 0 \tag{1}$$

where k is thermal conductivity, A_w the cross-sectional area, T the wall temperature, h_o the outside convection heat transfer coefficient, P_o the outside perimeter, T_∞ the surrounding temperature, h_i the inside convection heat transfer coefficient, P_i the perimeter of the vapor space, and T_v the inside vapor temperature.

The nondimensional temperature and length were defined as

$$\theta = (T - T_\infty)/(T_b - T_\infty), \qquad X = x/L \tag{2}$$

where L is the length of the heat pipe and T_b is the fin base temperature. Equation (1) was rewritten in terms of the nondimensional variables to give

$$\frac{\partial^2 \theta}{\partial X^2} - Z^2 \theta = -N^2 \theta_v \tag{3}$$

where

$$M^2 = \frac{h_o P_o L^2}{kA_w} \tag{4}$$

$$N^2 = \frac{h_i P_i L^2}{kA_w} \tag{5}$$

$$Z^2 = M^2 + N^2 \tag{6}$$

$$\theta_v = (T_v - T_\infty)/(T_b - T_\infty) \tag{7}$$

Equation (3) was then solved for $\theta(X)$. Assuming T_∞, T_v, h_i, and h_o were constants, the solution was shown to be

$$\theta(X) = \left[1 - \left(\frac{N^2\theta_v}{Z^2}\right)\right] \frac{\cosh[Z(X-1)]}{\cosh(Z)} + \frac{N^2\theta_v}{Z^2} \tag{8}$$

$$\theta_v = \frac{\tanh(Z)}{Z + (N^2/Z^2)\,[\tanh(Z) - Z]} \tag{9}$$

Last, the fin efficiency was found. Efficiency is the heat transfer from the fin divided by the maximum heat transfer if the entire fin is maintained at the fin's base temperature. The efficiency was found from the expression

$$\eta = \frac{\int_0^L h_o P_o (T - T_\infty)\, dx}{h_o P_o L (T_b - T_\infty)} = \int_0^1 \theta\, dX \tag{10}$$

Evaluating Eq. (10) for the case of the heat pipe fin that is flush mounted against the object yielded

$$\eta_o = \frac{\tanh(Z)}{Z + (N^2/Z^2)[\tanh(Z) - Z]} \tag{11}$$

A possible method of improving energy transport into the heat pipe fin would be to insert the heat pipe evaporator into the object. This would result in increased area for conduction to the evaporator. Figure 1 illustrates the difference between the flush-mounted and the inserted heat pipe fins. Next the efficiency of the inserted heat pipe fin will be found.

Inserted Heat Pipe Fin Analytical Results

The efficiency for the inserted heat pipe fin is also defined by Eq. (10). To find the efficiency, first the temperature distribution along the heat pipe must be found. Inserting the heat pipe into the object will influence the temperature distribution along the length of the heat pipe as well as the vapor temperature inside the heat pipe. For this work, it will be assumed that for $X \leq 0$ (inserted region) the heat pipe wall temperature is the same as the base temperature ($T = T_b$ or $\theta = 1.0$). For $X > 0$, Eq. (8) still gives the wall temperature. This is because the wall temperature is assumed to be the base temperature at $X = 0$. Before substituting Eq. (8) into Eq. (10) to find the efficiency, the new vapor temperature θ_v must be found. Equation (9) does not apply to the inserted heat pipe case. Bowman et al.[1] showed that the vapor temperature could be found by applying

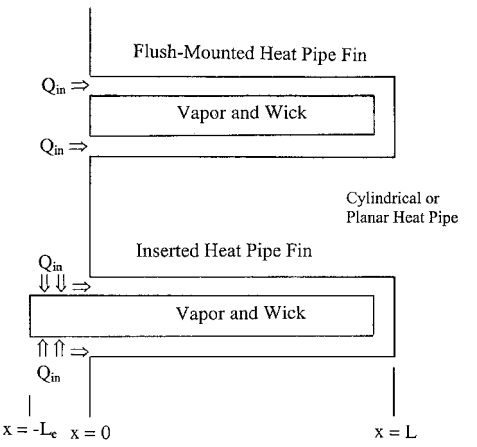

Fig. 1 Heat pipe fins studied.

Received 12 May 1999; revision received 23 August 1999; accepted for publication 25 August 1999.

*Associate Professor, Department of Mechanical Engineering. Senior Member AIAA.
†Research Assistant, Department of Mechanical Engineering.
‡Assistant Professor, Department of Mechanical Engineering. Member AIAA.

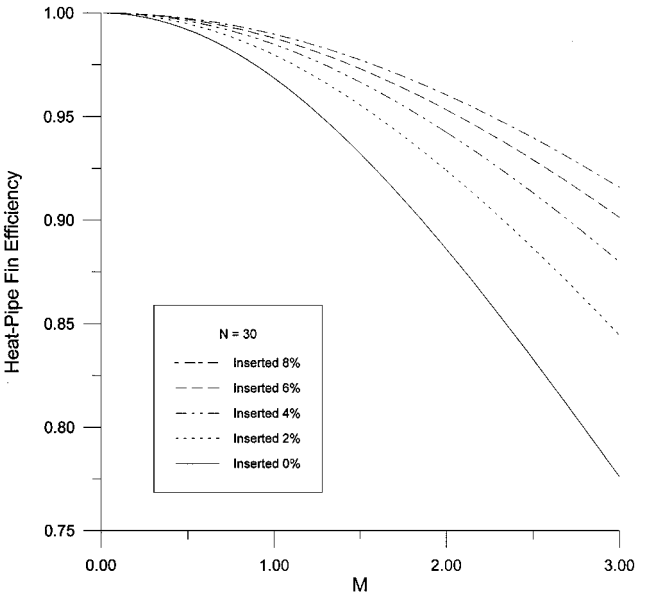

Fig. 2 Efficiency of inserted heat pipe fin.

conservation of energy to the vapor space. For the inserted heat pipe fin case, this results in the following expression:

$$\int_{-L_e}^{L} h_i P_i (T - T_v)\, \mathrm{d}x = \int_{-X_e}^{1} (\theta - \theta_v)\, \mathrm{d}X = 0 \qquad (12)$$

where X_e is the nondimensional length of the inserted portion of the heat pipe fin ($X_e = L_e/L$). Substituting the axial temperature distribution into Eq. (12) and then solving for the vapor temperature yields

$$\theta_v = \frac{\tanh(Z) + X_e Z}{(N^2/Z^2)[\tanh(Z) - Z] + (1 + X_e)Z} \qquad (13)$$

If Eqs. (8), (10), and (13) are combined, the efficiency of the inserted heat pipe fin can be found. After manipulation, the efficiency can be shown to be

$$\eta = \frac{\tanh(Z)}{Z} + \left[1 - \frac{\tanh(Z)}{Z}\right]\left(\frac{N^2}{Z^2}\right)\left\{\frac{\eta_o[X_e Z + \tanh(Z)]}{\eta_o X_e Z + \tanh(Z)}\right\} \qquad (14)$$

where η_o is the efficiency of the flush-mounted heat pipe fin given in Eq. (11)

The influence of inserting the heat pipe into the object is shown in Fig. 2. Figure 2 shows an example where $N = 30$. Inserting the heat pipe into the object can be seen to greatly improve the fin efficiency over the flush-mounted heat pipe case. The increase in efficiency is due to improved heat transfer into the evaporator region of the heat pipe. These are not surprising results. The value of this research is in the equations that were derived to predict the results. These simple equations make it easy to compare a heat pipe fin to a standard fin during the design process.

Equation (14) can also be used for the case where evaporation is also allowed from the end of the vapor space (which was assumed not to exist in the preceding derivation). The inserted length would need to be increased by a length equal to the area of the end of the vapor space divided by the perimeter of the inside of the heat pipe. This procedure is analogous to increasing a standard fin's length so that insulated fin tip results can be used when considering convection from the tip of the fin.[2]

Experimental Apparatus and Procedure

Flush-Mounted Heat Pipe Fin Experiments

The first experimental apparatus consisted of a copper plate with one standard fin and three heat pipe fins protruding from the surface. The plate was 10.2 cm square and 1.3 cm thick. A standard copper pin fin was silver soldered 6 mm into the plate. The fin was 8 mm in diameter and 26 cm long, leaving 25.4 cm of fin exposed to the ambient environment.

The three heat pipe fins mirrored the dimensions of the standard fin in length and outer diameter; however, they were constructed of 8-mm-o.d., 4.8-mm-i.d. copper tubing. Each heat pipe fin contained a copper screen wick (2.5 wraps, 100 mesh) and was filled with 2.8 ml of water. The finished wick measured 1.1 mm thick at the tube entrance but could have been as small as 0.5 mm thick (twice the screen thickness) if the layers were compressed inside the tubing. This thickness was one of the parameters needed to compare the experimental data to the analytical results. As was described in Ref. 1, $h_i = k_{\text{eff}}/t$, where k_{eff} is the effective thermal conductivity of the wick and t is the wick thickness.

Instrumentation consisted of eight type-T, surface-mount thermocouples. The thermocouples were electrically isolated from each other and from the fin. They were connected to a data acquisition card in a differential mode.

Testing was conducted in two main phases, namely, base and tip measurements and distributed temperature measurements. The base and tip measurements were conducted by first instrumenting each of the four fins with a thermocouple near the tip of the fin, 1 cm from the end. Four thermocouples were also attached to the copper base plate near each fin. The base was then heated to 130–135°C. All data channels were then sampled for 15 s at a rate of 10 samples per second per channel. The ambient air temperature was also recorded. Five tests were conducted in this phase: one with the fins in the vertical position (evaporator down), three in the horizontal position at angles of 0-, 5-, and 10-deg favorable tilt from the horizontal, and one flipped 180 deg from the vertical position (evaporator up).

The distributed temperature measurement tests were conducted in a similar manner; however, for this series of testing, all eight thermocouples were attached to one fin at a time for the duration of each test. The solid fin was first tested at two horizontal positions (0- and 10-deg tilt), and then two tests were conducted in a vertical position. For comparison, identical testing was performed on one of the heat pipe fins.

Inserted Heat Pipe Experiments

A second experimental apparatus was constructed to measure the influence of inserting the heat pipe into the object. The second heat pipe fin was made from a common vacutube used for drawing blood. The vacutube was selected because of its low thermal conductivity compared with that of copper and because of the good seal obtained by the stopper. The vacutube had a total length of 0.131 m, a useful inside length of 0.106 m, an inside diameter of 0.014 m, and an outside diameter of 0.015 m. Three wraps of 100 mesh copper screen were inserted into the vacutube for the heat pipe wick. The final wick thickness was 0.7 mm. The mass of water in the vacutube heat pipe was 2.0 g.

The evaporator end of the heat pipe was inserted into hot water to simulate a uniform temperature boundary condition along the inserted region. The condenser was cooled by convection to air. During the experiment, the inserted length in the water was varied. Four thermocouples were used for this experiment. They measured the ambient air temperature, the water temperature, the fin base temperature, and the fin tip temperature. The fin base temperature was found to be equal to the water temperature. This was checked because the analytical results assumed a uniform temperature distribution along the inserted region.

Comparison of Analytical Predictions with Empirical Results

Flush-Mounted Heat Pipe Results

Analysis of the experimental data revealed that the observed temperature distribution of the standard fin closely follows that of the analytical solution. Figure 3 compares the experimental data with the analytical solution. Data from vertical (fin above the plate) and horizontal orientations are shown. The dotted line represents the analytical temperature distribution.

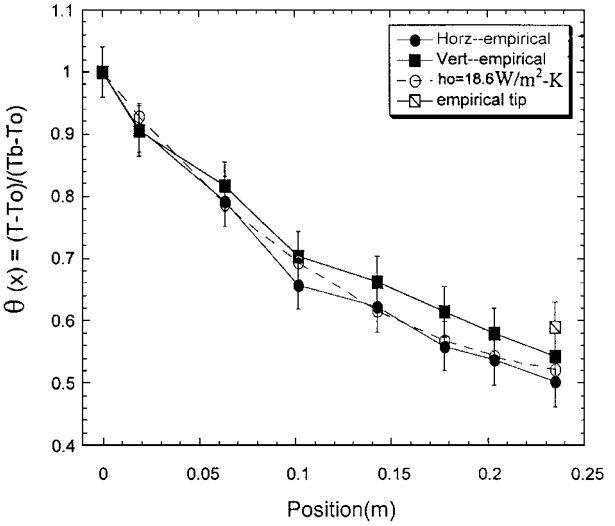

Fig. 3 Temperature distribution of the standard fin.

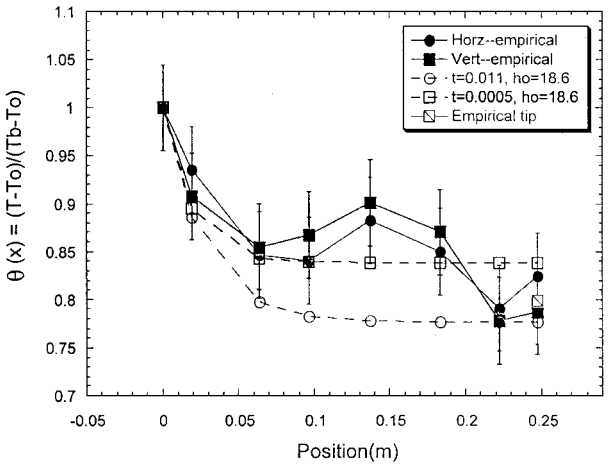

Fig. 4 Temperature distribution of heat pipe fin.

Besides validating the data acquisition system, the solid fin analysis helped quantify the fin convection environment. The convection heat transfer coefficient h_o was required to predict theoretical fin performance. It was thus necessary to find h_o from the standard fin data and use it in the analysis of the heat pipe fin. This appeared reasonable because all four of the fins were oriented alike and protruded the same distance from the copper base plate. The average fin tip temperature for the empirical tests was used as a means of finding the convection coefficient h_o from the fin. This was accomplished by varying h_o in the analytical solution until the analytical fin tip temperature matched the average empirical tip temperature. This resulted in a convection coefficient of $h_o = 18.6$ W/m^{2}K.

The analytical temperature distribution along the heat pipe fin is shown in Fig. 4. The two dotted lines in Fig. 4 refer to the analytical results for the two extreme wick thickness values, 1.1 and 0.5 mm. The measured temperature distribution (solid lines) follows the analytical solution within the uncertainty of the measurements.

With known analytical and experimental axial temperature distributions, efficiencies for both may be determined and compared. Table 1 presents efficiencies of the analytical solutions for standard and heat pipe fins, as well as calculated efficiencies from the empirical test results.

The measured efficiency of the standard fin was 5% higher when the fin was vertical than when it was horizontal. This difference may be due to the different convection environment. The vertical orientation, with the heated plate below the fin, would enhance free convection along the fin.

Table 1 Efficiencies

Position	Efficiency, % Analytical	Efficiency, % Empirical
	Standard fin	
Vertical	64	62 ± 2
Horizontal	64	57 ± 2
	Heat pipe fin	
Vertical	80–85	87 ± 3
Horizontal	80–85	89 ± 3

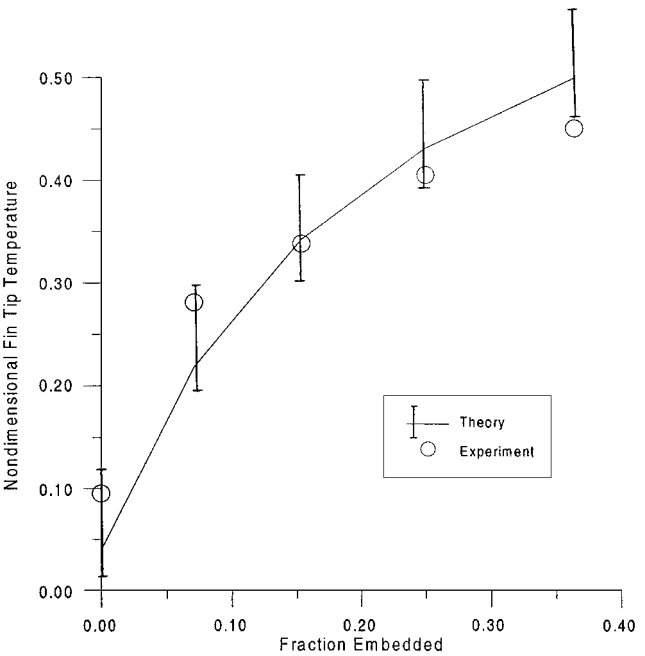

Fig. 5 Heat pipe tip temperature vs inserted length.

The heat pipe fin, on the other hand, seems to follow the opposite trend. In the vertical position, gravity causes any excess water to puddle in the bottom of the pipe. This adverse effect would lower the efficiency of the heat pipe fin. In the horizontal position, puddling effects are less of a factor. The horizontal orientation appears to yield an increase in efficiency; however, note that if error limits are considered the two heat pipe fin orientations could yield similar or even opposite results. The close efficiency values for the two orientations suggest that puddling was not a large factor.

As was mentioned earlier, one test was conducted with the evaporator above the condenser. During this test, evaporator dryout was observed. The heat pipe fin tip nondimensional temperature dropped from 0.82 (nondryout case) to 0.47 (dryout). With the evaporator dry, the heat pipe fin was less efficient than the standard fin.

Inserted Heat Pipe Results

The results from the tests with the second experimental apparatus (vacutube heat pipes) are shown in Fig. 5. These results were obtained by varying the amount of the heat pipe inserted in hot water. The tip and base temperature of the heat pipe as well as the environment temperature were monitored. Figure 5 compares the experimental results with the theory [Eqs. (8) and (13)]. The agreement between the experiment and the theory is good. The uncertainty is attached to the theoretical results. To predict the theoretical results, several experimentally determined parameters were needed. The most difficult to approximate were the outside and the inside convection heat transfer coefficients. The uncertainty limits shown reflect the high and low estimates for each of these parameters.

Inserting the heat pipe fin into the object that is being cooled has a large impact on the tip temperature of the fin and, thus, on the fin efficiency.

Conclusions

Expressions for the analytical temperature distribution and efficiency of a heat pipe fin were derived and compared with experimental data. Two heat pipe fin cases were studied, flush mounted and inserted into the object. The derived expressions are useful as a design tool. They allow the designer to compare heat pipe fins to standard fins before doing a detailed heat pipe design.

Further research could focus on variations in heat pipe design and geometry. These could include nonconstant properties and boundary conditions. For this work, the wall cross-sectional area, the internal convection coefficient, and the external convection coefficient were assumed constant. The impact of these assumptions on accuracy should be investigated. It would also be interesting to extend the analysis to fins in radiation environments.

References

[1]Bowman, W. J., Storey, J. K., and Svenson, K. I., "Analytical Comparison of Standard and Heat Pipe Fins," AIAA Paper 99-0475, Jan. 1999.

[2]Incropera, F. P., and DeWitt, D. P., *Fundamentals of Heat and Mass Transfer*, 4th ed., Wiley, New York, 1996, p. 122.

Forced Convection Heat Transfer to Phase Change Material Slurries in Circular Ducts

Edwin L. Alisetti* and Sanjay K. Roy†
University of Miami, Coral Gables, Florida 33124-0624

Introduction

PHASE change material (PCM) slurries are being considered for use in temperature control and thermal energy storage systems. However, theoretical models for heat transfer in such slurries have received relatively little attention. Chen and Chen[1] used a Dirac δ-function-based analytical model and a perturbation method to investigate the augmentation of heat transfer for a steady, laminar PCM slurry flow above a flat plate with constant wall temperature. Charunyakorn et al.[2] developed a numerical model for heat transfer to PCM slurries for flows between parallel plates and in circular ducts for various boundary conditions. Goel et al.[3] conducted an experimental study to verify the model of Charunyakorn et al.[2] for the case of flow in a circular tube with a constant heat flux boundary condition. They found that the experimental results agreed only qualitatively with the numerical prediction, with the difference between the two being of the order of 45%. Zhang and Faghri[4] modified the model of Charunyakorn et al.[2] to include the effects of the crust of the microcapsules, initial subcooling, and the width of the phase change temperature range. They found that the differences between their numerical results and the experimental results of Goel et al.[3] could be reduced or eliminated entirely by incorporating these three effects in the Charunyakorn et al.[2] model.

Previous theoretical models use a complicated source term or special analytical techniques so that they cannot be readily used in commercial computational fluid dynamics (CFD) packages. Also, when the phase change process occurs over a finite temperature range (for example, with multicomponent substances), the effective specific heat of the material may vary as a function of temperature. The effects of this variation on the heat transfer process have not been investigated to date. To overcome these limitations, an effective specific heat capacity model for heat transfer to a PCM slurry is presented. This model does not include a source term and is more easily implemented in standard CFD packages. Instead, various forms of the specific heat functions have been considered to account for the phase change effects, and numerical results have been obtained using the model.

Model Formulation

It is advantageous to consider a standard problem at this stage because the primary goal is to develop and to evaluate a new model for heat transfer with PCM slurries. Once the model verification is complete, it will be possible to use it to study more complex heat transfer processes as required. Thus, the problem of laminar heat transfer to a PCM slurry flowing in a circular duct with constant wall temperature T_w is considered in this Note. The flow is assumed to be fully developed, and the slurry enters the heated section at a temperature T_i that is equal to or below the melting point of the PCM. The volumetric concentration of the suspended PCM is less than 20–25% so that the flow is essentially Newtonian. The density of the PCM in both the liquid and solid phases is approximately equal to that of the suspending fluid so that the particles can be assumed to be neutrally buoyant and the slurry density can be treated as constant. The sizes of the PCM particles are much smaller than the radius r_0 of the tube so that the suspension behaves as a homogeneous fluid and the effects of the particle free layer next to the wall are negligible. The flow rate (with mean velocity U_m) is assumed to be sufficiently high so that there is no separation of the slurry constituents but is low enough so that viscous dissipation and axial conduction effects are negligible. Note that the basic assumptions here are similar to those used in previous studies.[2,4]

Based on the preceding description of the model, a simplified form of the energy equation is used to model the heat transfer process. The phase change effects are included in the energy equation through the specific heat capacity of the slurry, which is taken as a function of temperature. The thermal conductivity k_e is also taken as a function of the radial position to account for microconvective effects induced by the PCM particles suspended in the fluid. The energy equation can, therefore, be written as

$$2 \cdot Cp \cdot \rho \cdot U_m \left[1 - \left(\frac{r}{r_0}\right)^2\right] \frac{\partial T}{\partial x} = \frac{1}{r}\frac{\partial}{\partial r}\left(r \cdot k_e \frac{\partial T}{\partial r}\right) = \frac{1}{r}\frac{\partial}{\partial r}\left(r \cdot f \cdot k_b \frac{\partial T}{\partial r}\right) \tag{1}$$

with the following initial and boundary conditions:

$$T = T_i \quad \text{at} \quad x = 0, \qquad \frac{\partial T}{\partial r} = 0 \quad \text{at} \quad r = 0$$

$$T = T_w \quad \text{at} \quad r = r_0 \tag{2}$$

where k_b is the static bulk thermal conductivity and f is the microconvection-related enhancement factor that has been represented by piecewise linear functions[5] based on the general relation developed by Charunyakorn et al.[2]

The specific heat function must be derived carefully because it is the main part of this new model. As a first step, it is assumed that the specific heat capacity of the PCM, Cp_s, is the same in both the solid and liquid phases. Thus, in the absence of phase change, the specific heat of the slurry, Cp_{wo}, is calculated by using the mass fraction Cm of the PCM:

$$Cp = Cp_{wo} = Cm \cdot Cp_s + (1 - Cm) \cdot Cp_f \tag{3}$$

During the phase change process, the effective specific heat of the PCM will be a function of temperature (Fig. 1). In this temperature range, the effective specific heat $Cp = Cp_{sl}$ can be related to the latent heat h_{fs} by the following equation:

$$h_{fs} = \int_{T_1}^{T_2} Cp_{sl} \cdot dT \tag{4}$$

Four different specific heat functions have been considered in the present work. To represent symmetric distributions, rectangles and sinusoidal curves were chosen, whereas two oppositely oriented

Received 18 June 1999; revision received 13 September 1999; accepted for publication 15 September 1999.

*Graduate Student.

†Adjunct Associate Professor, Department of Mechanical Engineering.